

## Mineralogical and gemmological characteristics of garnets associated with xenoliths within trachyte dome, Hisarlıkaya (Ankara), Central Anatolia, Turkey

Elif VAROL<sup>1\*</sup>, Sibel TATAR ERKÜL<sup>2</sup>, Güllü Deniz DOĞAN KÜLAHCI<sup>1</sup>

<sup>1</sup>Department of Geological Engineering, Faculty of Engineering, Hacettepe University, Ankara, Turkey

<sup>2</sup>Department of Geological Engineering, Faculty of Engineering, Akdeniz University, Antalya, Turkey

Received: 15.06.2020 • Accepted/Published Online: 11.02.2021 • Final Version: 17.05.2021

**Abstract:** Garnet-bearing xenoliths are observed within a trachytic dome extrusion in the Hisarlıkaya region (Ankara). These garnets exhibiting greenish-reddish-dark brown colour and ranging in sizes up to 1 cm were examined in terms of mineralogical, geochemical, and gemmological characteristics. Mineralogical studies indicate that these garnets (And<sub>88-93</sub>Grs<sub>7-12</sub>) are linked to solid solution series, which are dominantly andradite with lower content of grossular. According to major, trace, and rare earth element (REE) analysis, the representative garnet crystal shows high CaO, Fe<sub>2</sub>O<sub>3</sub>, Al<sub>2</sub>O<sub>3</sub>, MgO, MnO, V, W, and light rare earth elements (LREE) concentrations. These high concentrations might indicate the mobility of these elements during skarn formation related with contact metamorphism, material exchange occurring via hydrothermal fluids, site geometry of the crystal, ionic radius of cations, and charge balance.

The Hisarlıkaya garnets display dodecahedron-trapezohedron crystal habits with good translucency, glassy, transparent features, and also optical isotropic character. Their refractive indices are high (>1.78), and specific gravities range from 3.66 to 3.67 g/cm<sup>3</sup>. These garnets are not suitable for use as gemstones since they cannot be cut or processed considering all the mineralogical properties of garnets.

**Key words:** Trachyte, xenolith, skarn, garnet, mineralogy, gemmology

### 1. Introduction

Garnets are a group of silicate minerals with different species such as pyrope, almandine, spessartine, grossular, uvarovite, and andradite that have similar physical properties, crystal structures, and different chemical compositions. Andradite [Ca<sub>3</sub>Fe<sup>3+</sup><sub>2</sub>(SiO<sub>4</sub>)<sub>3</sub>] is one of these species of garnets bearing calcium and iron elements, which can be commonly observed in titanium-rich chlorite schists, serpentinites, carbonatites (Ramasamy, 1986; Dietl, 1999; Stubna et al., 2019), and alkali magmatic rocks (Gomes, 1969; Deer et al., 1992; Gwalani et al., 2000; Adamo et al., 2011). Additionally, andradite is a typical mineral in skarns developing in contact metamorphic zones associated with magmatic intrusions into carbonate rocks. This mineral is of particular importance to obtain much geochemical and petrogenetic information, such as: (i) exploration of their chemical composition, (ii) their paragenetic relationships with other minerals, (iii) gemmological assessment, (iv) metasomatic fluids and sources, (v) mobility of elements during metamorphism, (vi) oxygen fugacity of hydrothermal fluids, and (vii)

determination of types of the skarn deposits (Dingwell and Brearley, 1985; Jamtveit and Andersen, 1992; Amthauer and Rossmann, 1998; Russell et al., 1999; Adamo et al., 2011; Schmitt et al., 2019; Fei et al., 2019).

The Hisarlıkaya region is a key area where xenoliths belonging to metamorphosed basement rocks are intensely observed. They were altered in the contact aureole of a magmatic intrusion into clayey-, calcareous- and sandy basement rocks. Xenoliths are observed in the trachytic rocks and might have been transported to the earth's surface by these volcanic rocks outcropping as a dome in the region. The studied garnet crystals exist in these xenoliths of skarn zone caused by contact metamorphism. These garnets vary from mm-cm in size within these xenoliths with cm-dm size, are well-preserved, and have reddish, brownish, and greenish colours. This study aimed to determine the types and composition of these garnets, to reveal their mineralogical, geochemical and gemmological characteristics and the usability of these crystals as gemstones. For this purpose, X-ray diffractometer (XRD), energy-dispersive electron microprobe analysis

\* Correspondence: elvarol@hacettepe.edu.tr

(EMPA-EDS), confocal Raman spectrometer (CRS), ultraviolet-visible and near-infrared (UV-VIS-NIR) spectrometer, and inductively coupled plasma-optical emission spectrometer/mass spectrometer (ICP-ES/MS) analyses were conducted. Gemmological standard testing (refractive index, colour, luster, and sheen test, Gemmo-FTIR analyses, optical absorption spectrum) was also performed on three single-crystal garnets.

## 2. Geological setting and sample description

The study area is located in the northern section of the İzmir-Ankara-Erzincan Suture Zone bounded by the Sakarya Block to the north, the Menderes-Tauride Block to the west, and the Kırşehir Block to the east (Figures 1a, 1b). Basement rocks comprise an ophiolitic melange containing Jurassic-Cretaceous limestone, sandstone, and shale mega blocks overlain by Upper Maastrichtian limestones and Palaeocene conglomerates, sandstone, limestone, and shale units (Koçyiğit and Lünel, 1987; Rojay and Süzen, 1997). Above these units, there are widespread alkaline and calc-alkaline composition volcanic rocks, active from the Miocene to the Pliocene. These are overlaid by sedimentary unit coeval with volcanism (Keller et al., 1992; Notsu et al., 1995; Wilson et al., 1997; Alıcı et al. 1998, Alıcı Şen et al., 2002; Tankut et al., 1998; Temel, 2001; Temel et al., 2010; Varol et al., 2007, 2008, 2014).

Volcanic rocks situated 45 km from Ankara city center crop out between Hisarlıkaya and Balkuyumcu districts. These rocks varying from basaltic to rhyolitic character are observed as a trachytic dome in the study area (Figure 2a) (Varol et al., 2007). The presence of xenoliths within this dome, located in the northwest of Hisarlıkaya district, is remarkable. They do not show any genetic relationship with the trachytic volcanic rocks. These xenoliths, which could not be melted during magma storage, might be formed by the intrusion of magma into the basement rocks.

The volcanic rocks contain many different types of xenoliths described during field and with mineralogical studies. These xenoliths are considered to have been fragmented from a contact aureole forming in basement rocks due to metasomatism linked to an intrusion with unknown size and shape. They have cm-dm size, and their shapes vary from round to angular. They are very common in a narrow area within the trachytic dome. The garnet crystals in these xenoliths are observed in two different forms in the field; i) across the boundaries of basement rock fragments as small crystals developing by the assimilation process during their upward transport by the magma (Figure 2b), and ii) in xenoliths fragmented from the contact aureole (Figures 2c, 2d). Garnet crystals found in coarser sizes (mm-cm) in xenoliths of skarn zone have a glassy-resinous luster and appear as garnet clusters

with mainly reddish-brown and occasionally greenish colours (Figures 2b-2f). The typical assemblage for the garnet-bearing xenoliths is garnet+pyroxene±plagioclase (Figures 2g, 2h).

## 3. Materials and methods

Thirteen xenolith samples consisting of garnet crystals were collected from the study area (Figures 2a-2d). Many crystals of various number and sizes were separated from these xenoliths (Figure 2e). Different spectroscopic, geochemical, and optical methods were performed on three euhedral single-crystal representative garnets with cm diameter (samples; Gr-1, Gr-2, Gr-3) (Figures 2f-2h). Garnets were placed in an ultrasonic bath for 120 min, at 500 °C in 10% HCl acid, and then washed three times with distilled water. The cleaned-samples were ground at Hacettepe University Crushing-Grinding Laboratory (Ankara, Turkey).

The chemical composition of garnets was determined at Middle East Technical University-Central Laboratory (METU-MERLAB, Ankara, Turkey) using via a JXA-8230 Electron Probe Microanalysis (EPMA) device, operated at 15 kV accelerating voltage, 20 nA beam current with a beam diameter of 5 µm, and an integrated 1.2 nm high-resolution QUANTA 400F field emission scanning electron microscope (SEM).

XRD measurements were performed on the powdered-samples of xenoliths and single-crystal garnets using a Rigaku D/MAX-2200 X-ray diffractometer with CuK $\alpha$  radiation in the Department of Geological Engineering of Hacettepe University (Ankara, Turkey). The samples were scanned over 2 $\theta$ , which ranges from 2 to 70° with a tube voltage of 40 kV and tube current of 40 mA.

Detailed characterization of garnet crystals was carried out with a Thermo Scientific, DXR-2 Confocal Raman Spectrometer (CRS) in Ankara University YEBİM Laboratory (Ankara, Turkey). These analyses were obtained using transmitting laser at 633 nm wavelength, and Raman shift spectra were obtained in 100-1200 cm<sup>-1</sup> interval.

UV VIS-NIR characteristics for three single-crystal garnets were performed at Çukurova University Central Laboratories (Adana, Turkey) with an Agilent Cary 7000 Universal Measurement Spectrophotometer (UMS) applying 280-1100 nm wavelengths.

Major, trace, and rare earth element geochemical analysis of one single-crystal of garnet (sample Gr-1) were performed in Acme Analytical Laboratories (Vancouver, Canada). The sample was mixed with LiBO<sub>2</sub> (lithium metaborate). Major element contents in the sample were measured with ICP-ES using the fusion method and trace element contents were measured with ICP-MS using the HNO<sub>3</sub> (nitric acid) digestion method after the fusion method.

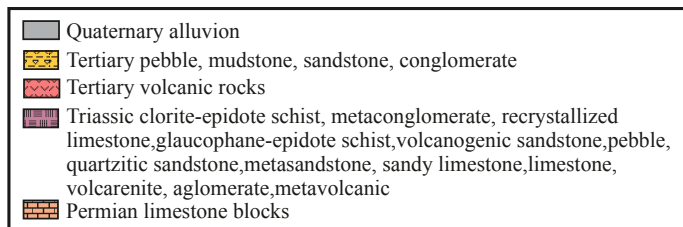
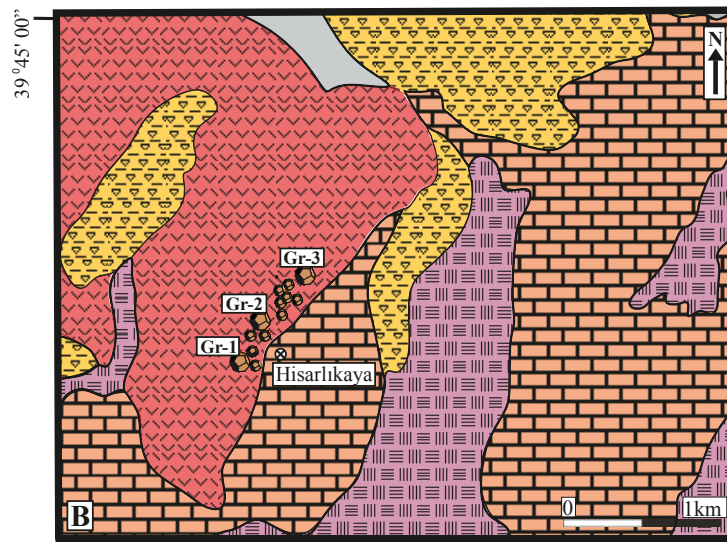
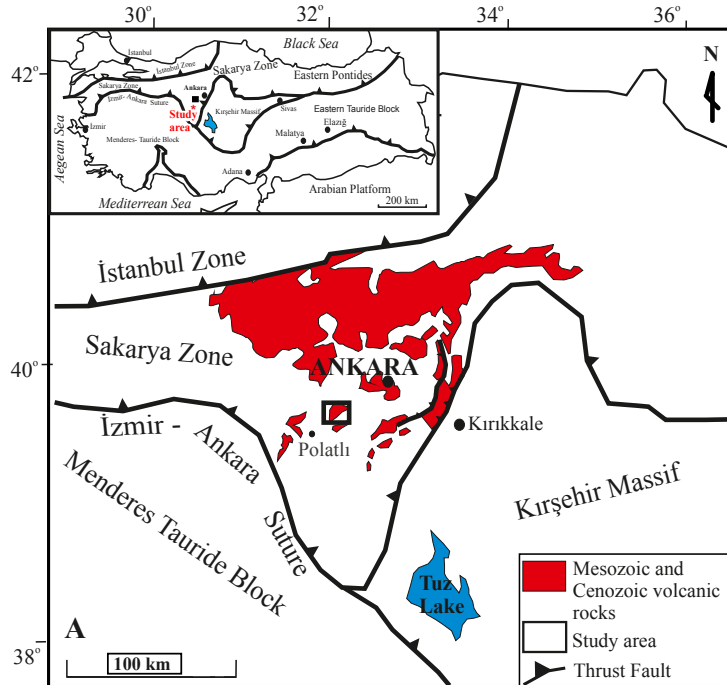


**Figure 1.** a) Simplified map of the main tectonic units (from Okay and Tüysüz, 1999) showing the study area and Mesozoic and Cenozoic volcanic rocks around Ankara. b) Geological map of the Hisarlıkaya area (modified from Akyürek et al., 1995) and the locations of the xenoliths (Gr-1, Gr-2, Gr-3 are the analysed single-crystal samples of garnet separated from xenoliths).

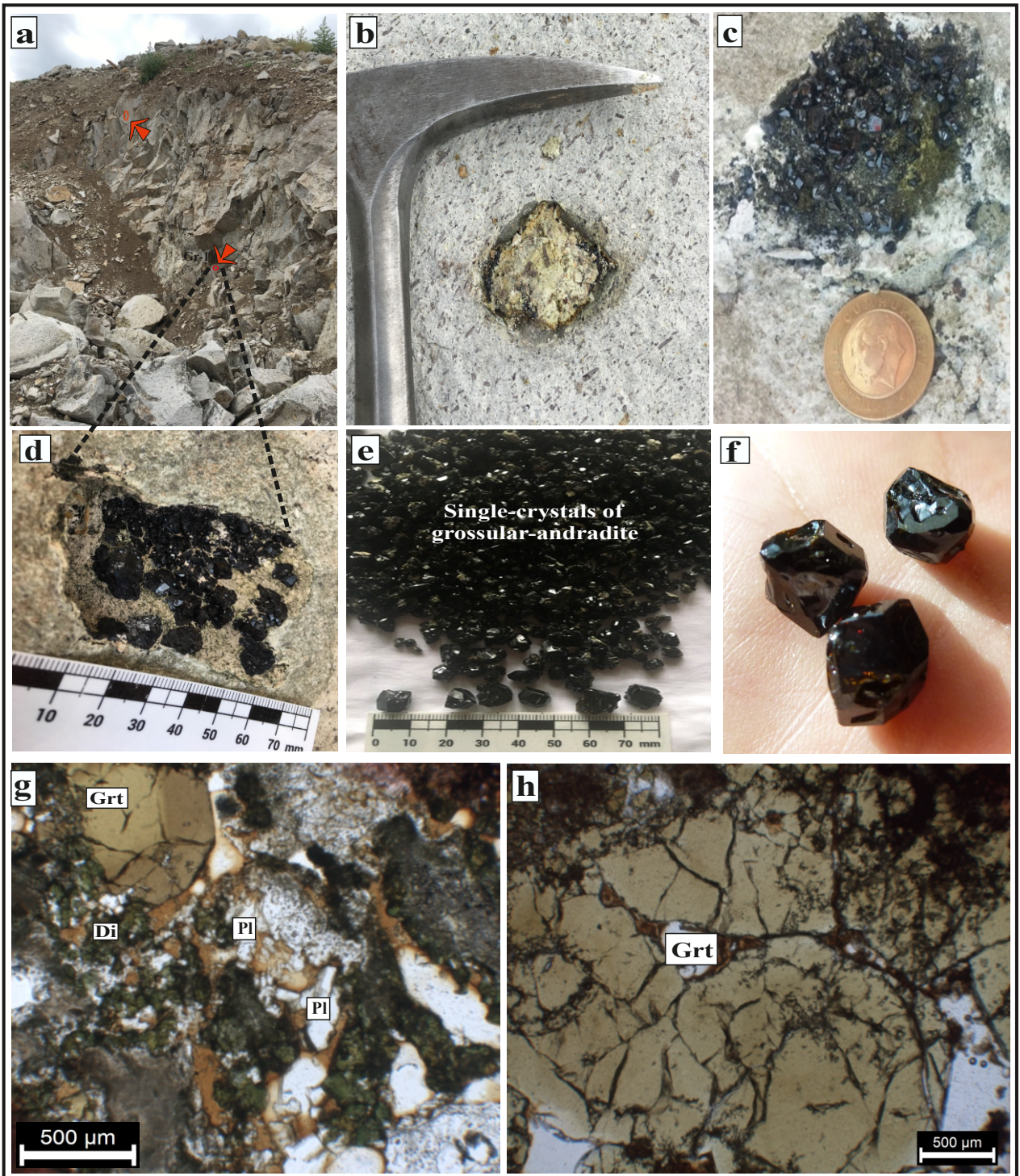


**Figure 2.** a) A representative general view of Hisarlıkaya trachytic volcanic rocks and the xenoliths they contain. b) Garnets formed across the boundaries of basement rock fragments. c, d) Representative garnet-bearing xenolith samples from Hisarlıkaya. e) Single-crystals of grossular-andradite up to 1.0 cm shelled from the xenoliths. f) The analysed single-crystal samples. g, h) Microphotographs of representative xenoliths bearing garnet crystals from Hisarlıkaya xenoliths (Grt: garnet, Di: Diopside, Pl: Plagioclase) (parallel nicol).

Standard gemmological analyses were performed in the Gemmology Laboratory of the General Directorate

of Mineral Research and Exploration (MTA) (Ankara, Turkey) using Eickhorst polariscope, refractometer,

and optical absorption spectrometer. Gemmological analyses identify the optical characters, refractive indexes transparencies, and specific gravities of the minerals. Spectra for three sample crystals were also obtained by a Magilabs Gemmo-FTIR device in the wavelength interval 450-1800  $\text{cm}^{-1}$ .

We determined that these three samples have similar physical properties, crystal forms, and same spectroscopic characteristics based on the aforementioned analytical methods. We chose to present analytical results for only one sample here (Figures 3, 4) due to the similarity of the mineralogical spectra for all three samples.

#### 4. Results

##### 4.1. Mineralogical and geochemical characteristics

##### 4.1.1. Energy-dispersive spectroscopy - electron micro-probe analysis (EDS- EMPA)

EDS-EMPA analysis and calculation results for garnet crystals are given in Table 1. With the general chemical formula  $\text{X}_3\text{Y}_2(\text{SiO}_4)_3$ , garnet group minerals invariably contain Ca in addition to Mg,  $\text{Fe}^{2+}$ , and Mn at the dodecahedral X site, while  $\text{Fe}^{3+}$ , Al, Cr, and Ti are found at the octahedral Y site and  $\text{SiO}_4$  at the tetrahedral Z site (Kolesov and Geiger, 1998; Geiger and Rossman, 2018).

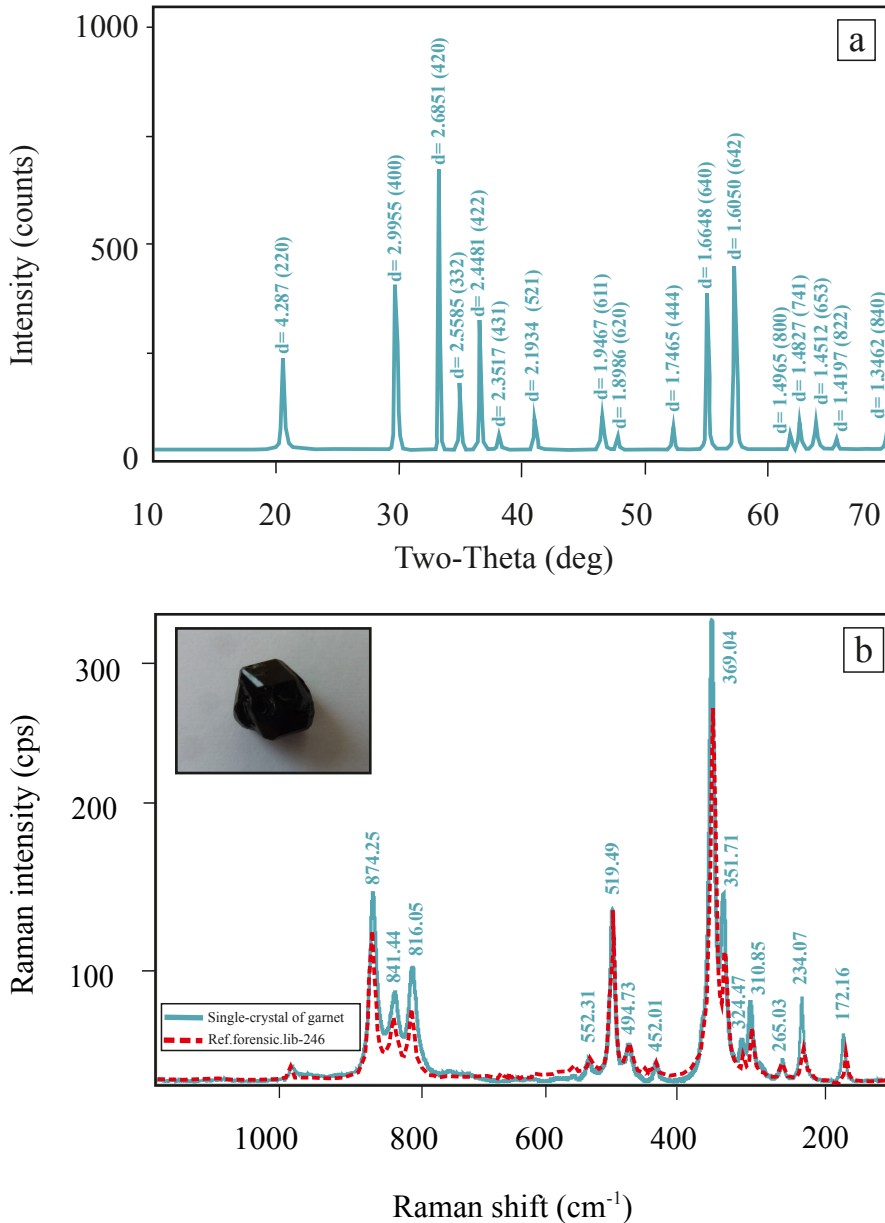


**Figure 3.** a) Powder X-ray diffraction pattern, b) Confocal Raman characteristics of Hisarlıkaya garnet crystals.

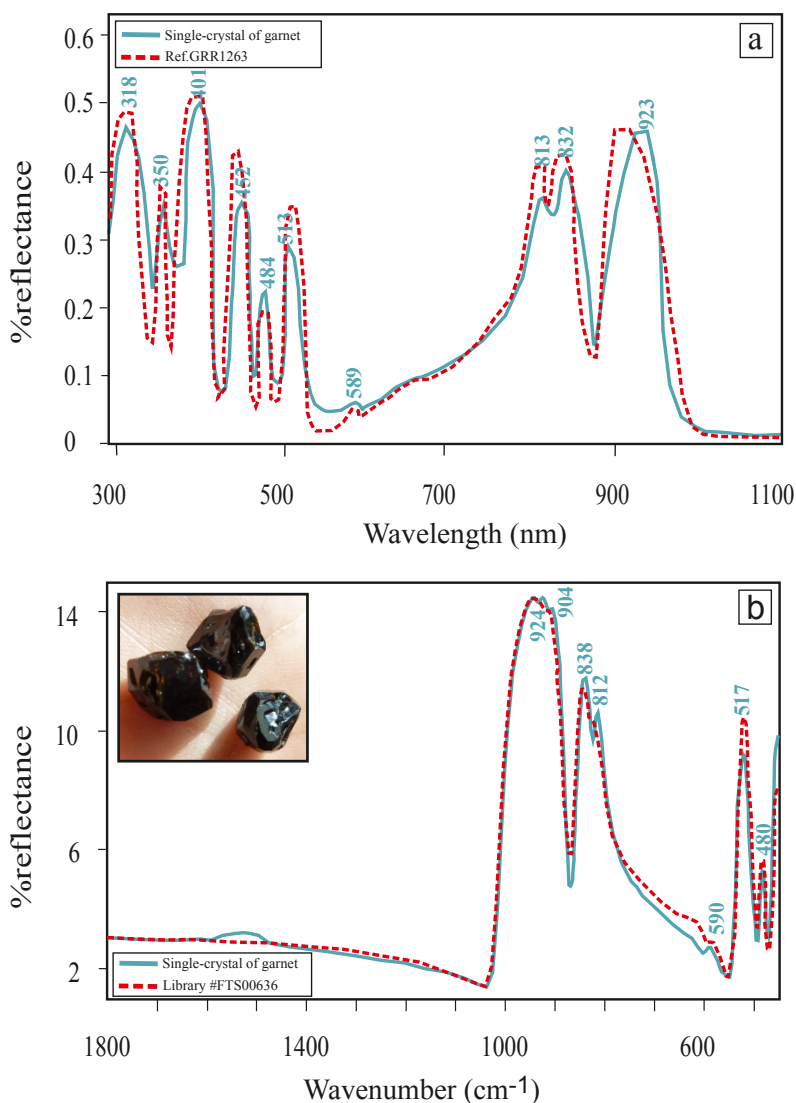


**Figure 4.** a) Infrared (IR), b) Fourier transform infrared spectrophotometer (FTIR) characteristics of Hisarlıkaya garnet crystals.

According to analysis results, noting stoichiometry and charge balance, the measured chemistry for the garnet samples was calculated as  $(Ca_{2.93}Mg_{0.03}Fe^{2+}_{0.02}Mn_{0.02})_{\Sigma=3}(Fe^{3+}_{1.70}Al_{0.21}Ti_{0.09})_{\Sigma=2}(Si_{1.00}O_4)_3$  based on 12 anions. The calculations show that the crystals are andradite-grossular solid solution series with composition generally of high % andradite content in addition to lower grossular content ( $Adr_{88-93}Grs_{7-12}$ ) (Table 1).

#### 4.1.2. X-ray diffraction spectra (XRD)

The structure and type of garnet crystals analysed with XRD was determined with the Jade software package (with a reference sample; 10-288) (Figure 3a). XRD spectra identification revealed the main crystal phase was andradite. The spectra obtained when crystals are

andradite-grossular solid solutions are similar to XRD spectra obtained from pure andradite crystals. This situation is stated to only cause an increase in intensity (Wang et al., 2019). Linked to this, the XRD spectra for Hisarlıkaya garnet crystals have overlapping andradite and grossular peaks, and it is only to be expected that the grossular presence determined in EMPA calculations is not defined in these spectra.

#### 4.1.3. Confocal Raman spectra (CRS)

Raman spectrum analyses were taken for garnet crystals in the 100-1200  $cm^{-1}$  interval (Figure 3b). The Raman spectra for the analysed garnet crystals were compared with the LabSpec software database (with a reference sample; forensic-lib-246). The crystals were compatible

**Table 1.** Electron microprobe analyses for samples of garnet crystal from Hisarlıkaya region with formula calculated based on 12 oxygen atoms and garnet end-members proportions. (r: rim, c: center)

	Gr-1			Gr-2		Gr-3
	#1	#2	#3	#4	#5	#6
	r→	c→	r	c	c→	r
SiO <sub>2</sub>	35.48	36.12	35.77	35.40	35.18	35.01
TiO <sub>2</sub>	1.26	0.15	1.29	1.25	1.69	1.53
Al <sub>2</sub> O <sub>3</sub>	2.00	2.27	2.04	2.61	2.38	1.46
Fe <sub>2</sub> O <sub>3</sub>	26.58	26.45	26.44	25.79	25.79	25.96
MnO	0.44	0.50	0.43	0.27	0.44	0.33
MgO	0.25	0.33	0.28	0.20	0.20	0.36
CaO	32.08	31.54	32.40	32.68	32.45	32.81
Cr <sub>2</sub> O <sub>3</sub>	0.02	0.04	0.04	0.05	0.03	0.03
Total	98.11	97.40	98.69	98.24	98.17	97.49
Si	3.008	3.072	3.013	2.992	2.979	2.997
Ti	0.080	0.010	0.082	0.079	0.108	0.098
Al	0.200	0.228	0.203	0.260	0.238	0.148
Fe	1.696	1.693	1.676	1.640	1.643	1.672
Mn	0.031	0.036	0.031	0.019	0.032	0.024
Mg	0.032	0.042	0.035	0.025	0.026	0.045
Ca	2.914	2.874	2.924	2.959	2.944	3.009
Cr	0.001	0.000	0.003	0.003	0.002	0.002
Total	7.963	7.957	7.965	7.977	7.972	7.994
Tetrahedral (Z) site						
Si	3.01	3.07	3.01	2.99	2.98	3.00
<sup>IV</sup> Al	0.00	0.00	0.00	0.01	0.02	0.00
Σ	3.01	3.07	3.01	3.00	3.00	3.00
Octahedral (Y) site						
<sup>VI</sup> Al	0.20	0.23	0.20	0.25	0.22	0.15
Ti	0.08	0.01	0.08	0.08	0.11	0.10
Fe <sup>III</sup>	1.67	1.65	1.67	1.64	1.64	1.67
Cr	0.00	0.00	0.00	0.00	0.00	0.00
Σ	1.95	1.89	1.95	1.98	1.98	1.92
Dodecahedral (X) site						
Mg	0.03	0.04	0.04	0.02	0.03	0.05
Mn	0.03	0.04	0.03	0.02	0.03	0.02
Ca	2.91	2.87	2.92	2.96	2.94	3.01
Fe <sup>II</sup>	0.02	0.05	0.01	0.00	0.00	0.00
Σ	3.00	3.00	3.00	3.00	3.00	3.08
Alm(%)	0.0	0.0	0.0	0.0	0.0	0.0
Prp(%)	1.07	1.41	1.18	0.82	0.86	1.48
Sps(%)	1.05	1.22	1.03	0.64	1.05	0.78
GAU(%)	97.88	97.37	97.79	98.54	98.09	97.75
Total	100.0	100.0	100.0	100.0	100.0	100.0
Grs(%)	9.2	10.7	9.4	12.0	10.9	7.0
Adr(%)	90.7	89.2	90.5	87.9	89.0	92.9
Uva(%)	0.1	0.1	0.1	0.1	0.1	0.1
Total	100.0	100.0	100.0	100.0	100.0	100.0

with the andradite spectrum patterns (Figure 3b). Raman spectra of Fe-Al garnets have relatively strong Raman peaks in three spectral regions: (1) low energy peaks between 160 to 415  $\text{cm}^{-1}$  (around 350  $\text{cm}^{-1}$ ), (2) medium energy peaks between 450 to 660  $\text{cm}^{-1}$  (around 550  $\text{cm}^{-1}$ ), and (3) high energy peaks between 815 to 1062  $\text{cm}^{-1}$  (around 900  $\text{cm}^{-1}$ ), which can be assigned to rotational, internal bending, and stretching vibrations of the  $\text{SiO}_4$  tetrahedra, respectively (Hofmeister and Chopelas, 1991; Kolesov and Geiger, 1998). The Raman frequencies for the garnet crystals separated from xenoliths were between 172.16  $\text{cm}^{-1}$ –874.25  $\text{cm}^{-1}$ . High peaks were obtained for 351.71–369.04  $\text{cm}^{-1}$ , 494.74–519.49  $\text{cm}^{-1}$  and 816.05–874.25  $\text{cm}^{-1}$  Raman shifts (Figure 3b). It was observed that the other bands had a lower intensity. The obtained spectra were determined to be consistent with andradite with high purity, as stated by Hofmeister and Chopelas (1991). The band at 172.16  $\text{cm}^{-1}$  is assigned to translation mode of the  $(\text{SiO}_4)^{4-}$  or (Ca) at the X site, bands between 310.85–369.04  $\text{cm}^{-1}$  are attributed to rotations of the  $[\text{SiO}_4]^{4-}$ , bands between 452.01–552.31  $\text{cm}^{-1}$  are peaks for Si–O bending motions within  $\text{SiO}_4$  groups, and bands at 816.05–874.25  $\text{cm}^{-1}$  can be attributed to Si–O stretching motions within  $\text{SiO}_4$  groups (Hofmeister and Chopelas, 1991; Kolesov and Geiger, 1998).

#### 4.1.4. Infrared spectrometry (IR spectra)

The Gemmo-FTIR and IR (Far-mid) reflectance spectra obtained from garnet crystals separated from xenoliths are given in Figures 4a, 4b. These spectra were observed to be compatible with each other. These crystalline silicate garnets appear to have characteristic IR reflectance for andradite species (with a reference sample; GRR1263) (Hofmeister and Chopelas, 1991). This garnet crystal was observed to have a typical peak for andradite at the near 320  $\text{cm}^{-1}$  band (Figure 4a). The band at 300  $\text{cm}^{-1}$  has a very intense peak, and the band at 350  $\text{cm}^{-1}$  has a more moderate peak assigned to  $\text{Fe}^{3+}$  that replaces  $\text{Al}^{3+}$  in the octahedral site (Hofmeister and Chopelas, 1991). The presence of these bands associated with  $\text{Fe}^{3+}$  (300  $\text{cm}^{-1}$  and near 350  $\text{cm}^{-1}$ ) in the octahedral site reveals a high % content of andradite in the crystals (Hofmeister and Chopelas, 1991).

The band values in garnets with pure andradite composition have nearly equal intensity values in the 400–477  $\text{cm}^{-1}$  interval (McAloon and Hofmeister, 1995). Andradite-grossular solid solution products have a lower intensity for the 450  $\text{cm}^{-1}$  bands (McAloon and Hofmeister, 1995). Evaluation of the peaks at bands obtained in the FT-IR and IR spectra showed that the sample crystals are andradite-grossular solid solution products (Figures 4a, 4b).

#### 4.1.5. Major and trace element geochemistry

The geochemical analysis results for one single-crystal of garnet are given in Table 2. The garnet mineral has high

CaO (31.70%),  $\text{Fe}_2\text{O}_3$  (29.09%),  $\text{Al}_2\text{O}_3$  (1.72%), MgO (0.29%), MnO (0.51%), V (760 ppm), W (782 ppm), LREE concentrations. Major element concentrations are similar to values obtained from the EMPA; however, Ti values are lower than the results of microprobe analyses. As seen from the microprobe analysis, Ti element concentrations display some variations based on different points in the crystals, but it does not represent the whole crystal composition. The lower Ti concentration in the center (0.15%) of the Gr-1 sample crystal was detected to be higher (1.26%–1.29%) at the sample rims. The difference between geochemical and microprobe analysis results might be related to the difference in Ti concentration depending on points measured in crystals. It can be concluded that different crystals can have different  $\text{TiO}_2$  concentrations. Chondrite-normalized multi-element diagram for the Hisarlıkaya garnet sample shows that the LREE (La to Gd) are enriched more than the HREE (Tb to Lu) (Figure 5). The  $\Sigma\text{REE}$  content and LREE/HREE ratios of garnet crystal are 70.6 ppm and generally higher than 1, respectively.

## 4.2. Gemmological characteristics

### 4.2.1. Gemmological standard tests

The three single garnet crystals, separated from the xenoliths, present dodecahedron-trapezohedron habits (Figures 6a–6d). Gemmological properties of these crystals are described as follows:

**Colour and sheen test:** The sample crystals are translucent, glassy, and transparent. The colour of crystals ranges from greenish to dark reddish-brown, and changes gradationally from core to rim. The center colour of the crystals is typically greenish and less transparent than the rims. Their rims are reddish-brown. These colour variations indicating compositional zoning are observed from the rims to the crystal cores (Figures 6a, 6c).

**Polariscope study:** The samples of garnet show single-refraction, they are all isotropic.

**Refractive index and specific gravity:** The refractive indices were measured using refractometer calibration solution ( $>1.78$ ) at the Gemmology Laboratory of MTA. RI values for the entire crystals are larger than 1.78. It is widely accepted that the grossular-andradite solid solution series has higher RI than grossular (1.73–1.76) and lower RI than andradite (1.85–1.89) (Johnson et al., 1995, Lacivita et al., 2013). The specific gravities (SG) of samples range from 3.66  $\text{g/cm}^3$  to 3.67  $\text{g/cm}^3$ . As the sample crystals were described as andradite-grossular solid solution series, the obtained RI and SG values are consistent with the properties of these type crystals (Johnson et al., 1995).

**Optical absorption spectroscopy:** The examined crystals show a band with a center ranging from 430 to 450 nm. This measurement is consistent with the typical spectrum of andradite, showing a dark band at 440 nm (Payne, 1981).

**Table 2.** Major, trace and rare earth element compositions of the garnet crystal (Gr-1) from Hisarlıkaya region. (DL = Detection Limit).

Garnet sample no: Gr-1			
SiO <sub>2</sub> (%)	35.99	Zr	29.5
CaO	31.70	La	11.4
Fe <sub>2</sub> O <sub>3</sub>	29.09	Ce	17.5
MnO	0.51	Pr	2.94
Al <sub>2</sub> O <sub>3</sub>	1.72	Nd	11.9
MgO	0.29	Sm	2.43
TiO <sub>2</sub>	0.17	Eu	0.58
Zn (ppm)	19	Gd	2.63
Sc	8	Tb	0.38
Co	49.3	Dy	2.05
Ga	11.4	Ho	0.44
Nb	27.0	Er	1.26
Sn	165	Tm	0.16
Cr	< DL	Yb	1.02
Th	2.8	Lu	0.15
U	70.2	Y	15.8
V	760	ΣREE	70.6
W	781.9		

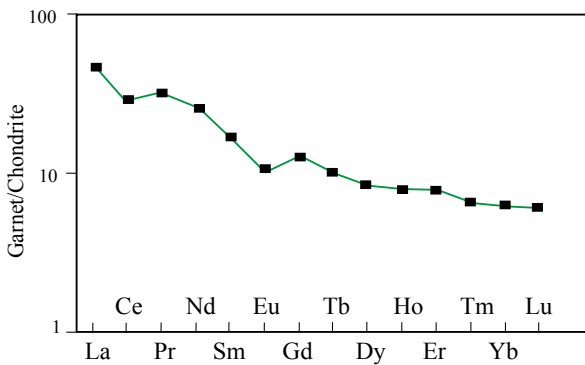


**Figure 5.** Chondrite-normalized (Anders and Grevesse, 1989) rare earth elements diagram for the garnet crystal (Sample no: Gr-1).

These gemmological characteristics are consistent with the identification of garnets as andradite species as suggested by O'Donoghue (2006) for the mineralogical and geochemical characteristics of gem garnet group.

#### 4.2.2. Processability

The studied garnet crystals crystallised at different dimensions from mm to cm size. Crystals are suitable for rose-shaped cabochon cutting by lapidaries. The rose cut features are a flat bottom with a dome-shaped

crown reaching an apex formed by three facets or more and this cutting style transitioned over to a few coloured gems, such as garnet since ancient times (e.g., Gilbertson, 2016). However, crystals broke during cutting process due to fractures and growth channels they contained. The Hisarlıkaya garnets may be considered as gemstones based on the mineralogical and gemmological characteristics. However, they are not suitable for cutting and also processing (>0.5 cm) as a gemstone due to fracturing/fragmentation.

#### 5. Discussion and conclusions

Garnet crystals are observed in xenoliths and at the boundary of basement rock fragments in a relatively limited area within a trachytic dome outcropping near Hisarlıkaya (Figures 2a-2d). Garnets which developed along the boundary of basement rock fragments assimilated by trachytic volcanic rocks are very fine-grained. Conversely, the garnets within the xenoliths have dimensions ranging from mm to cm sizes. These coarser garnets belong to the series of andradite-grossular solid solution (Table 1). According to the mineral assemblage of the xenoliths comprising andradite-grossular solid solution series +diopsidic clinopyroxene+ plagioclase, these garnet crystals were mainly formed in skarns during the prograde stage of the mineralisation process (Deer et al., 1992; Meinert et al., 2005; Jiang et al., 2018). This assemblage might be attributed to the mobility of elements during skarn formation, enrichment in some elements (Fe<sub>2</sub>O<sub>3</sub>, Al<sub>2</sub>O<sub>3</sub>, MgO, MnO, V, W, Sn, LREE, and ΣREE) by hydrothermal fluids during metasomatism, the bulk composition of the source magmas and/or wallrocks, temperature of the environment and to a lower extent pH value and pressure conditions (Russell et al., 1999, Raspar et al., 2008; Bocchio et al., 2010).

The enrichment or depletion of trace and REE are related to X and Y structural sites of garnet [X<sub>3</sub>Y<sub>2</sub>(SiO<sub>4</sub>)<sub>3</sub>] (Rubatto et al., 2020). The chondrite-normalized REE pattern for the Hisarlıkaya garnet presents an enrichment in LREE relative to HREE and a negative Eu anomaly. Bocchio et al. (2010) stated that Fe-rich garnets (andradite) enriched in LREE according to HREE and show positive Eu anomaly, while Al-rich garnets (grossular) had depletion in LREE according to HREE and negative Eu anomaly. Gaspar et al. (2008) mentioned additionally that Al-rich garnets have more ΣREE concentrations whereas Fe-rich garnets have much lower ΣREE concentrations. Accordingly, it is observed that the total REE content of the Hisarlıkaya Fe-rich garnet sample (Gr-1) is relatively low (70.6 ppm). The total content of REE may vary due to their concentrations in the source magmas and/or wall rocks or in the hydrothermal fluids (Gaspar et al., 2008).

The incorporation of trace and REE into garnet crystals is essentially controlled by crystal chemistry (Caporuscio

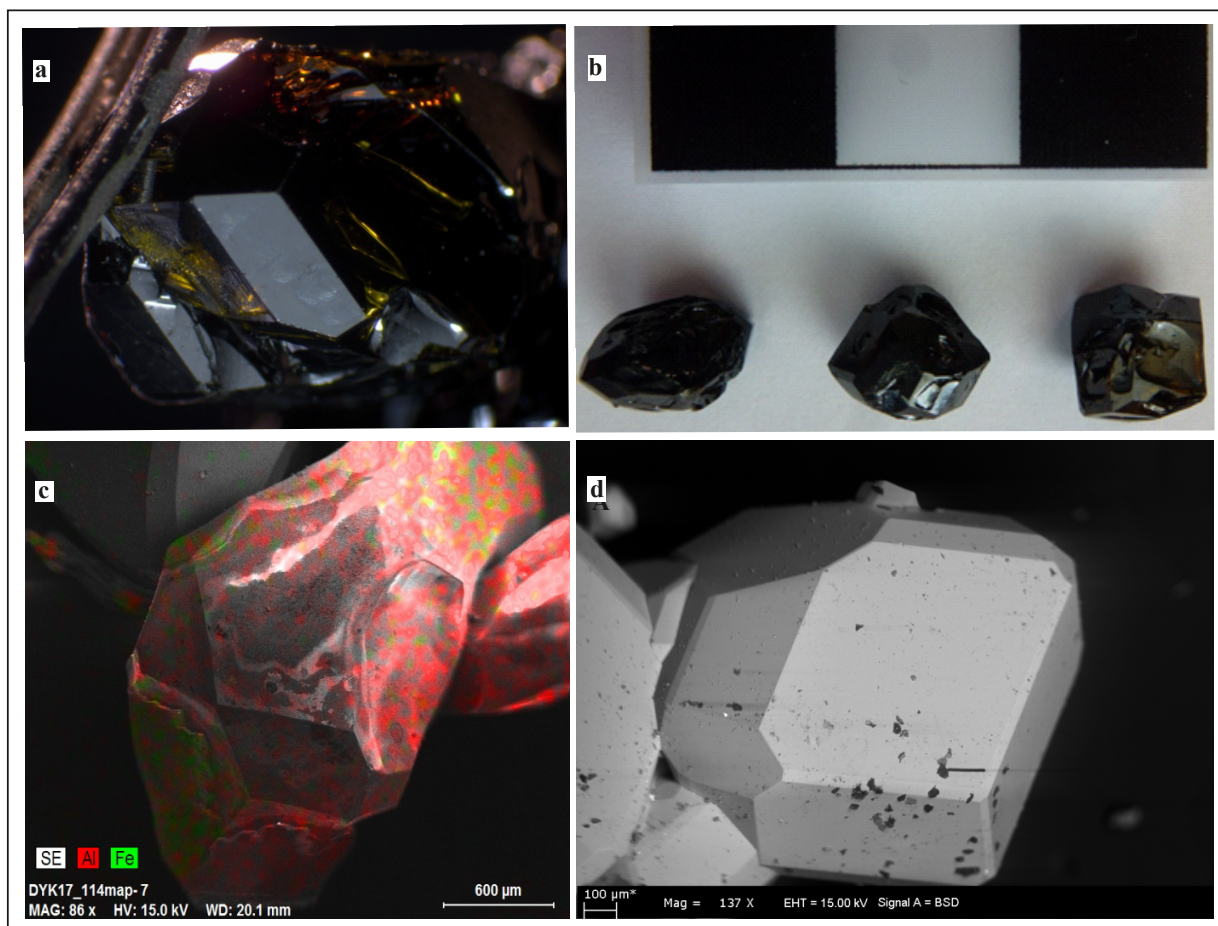


**Figure 6.** a) Gemmological microscopic image of andradite showing colour zoning. b) Garnet crystals up to 1.0 cm with dodecahedron-trapezohedron habits. c) Scanning electron microscope (SEM) image of garnet crystal showing Fe and Al compositional variation. d) SEM image of rhombic-truncated dodecahedron garnet crystal.

et al., 2019). This study also mentioned that the X site dimension plays a critical role in REE incorporation into the garnet structure. The X site dimension increases with increasing Ca content at the X site, and because of edge-sharing, increased Ca contents also correlate with increases in Y and Z sites dimensions (Caporuscio et al., 2019). Many researchers suggest that garnet can incorporate significant amounts of cations with large ionic radius that substitute for Ca at the X site because of the flexibility of the structure (Harte and Kirkley, 1997; Van Westrenen et al., 1999; Smit et al., 2014; Caporuscio et al., 2019). Shannon (1976) states also that the most important reasons for substitution of REE in skarn garnets is similarity between ionic radius of  $\text{Ca}^{2+}$  and trivalent REE in the dodecahedral X site. All these studies reveal that high Ca contents correlate with increasing trace and REE abundance with large ionic radii in the garnet structure. The Hisarlıkaya garnets have a composition of high % andradite content in addition to lower grossular content.

The cations incorporated in the studied garnet structure are dominantly Ca in the dodecahedral X site;  $\text{Fe}^{3+}$  in the octahedral Y site and Si in the tetrahedral Z site (Table 1). Geochemical analysis results for the Gr-1 sample displays high Ca content (31.70%). This circumstance could allow significant incorporation of REE with larger ionic radii and charges in the structure (i.e. LREE). Bocchio et al. (2010) also indicates that ionic radius of cations in the calcic garnets can be accommodated in X and Y sites increasing from grossular to uvarovite up to andradite. So, the larger cations like LREE can be more easily accommodated in the Hisarlıkaya garnet structure ( $\text{Adr}_{88-93}\text{Grs}_{7-12}$ ) than the smaller HREE due to the similarity of the ionic radius of Ca with LREE.

Compositional variability is detected in the mineralogical and geochemical studies due to the high % andradite and low % grossular contents of the Hisarlıkaya garnets ( $\text{Adr}_{88-93}\text{Grs}_{7-12}$ ). These variations in composition cause macroscopic and microscopic colour changes in the

garnet crystals and indicate zonation patterns (mineral zoning). The mineral zoning formed in the skarn zone with metasomatic processes is a crucial tool to determine chemical composition of hydrothermal fluids during mineralisation and may provide a continuous record of the physicochemical evolution of the hydrothermal system (Jamtveit et al., 1993; Zamanian et al., 2017). According to Meinert (1997), compositional zoning and colour changes in garnets from skarn deposits garnets can be observed systematically. The greenish to brownish colour changes from grossular rich cores to andradite rich rims in the Hisarlıkaya garnet crystals (Figure 6, Table 1) can be seen with naked eye with a gradual change of colour (Figures 2f, 6a). Krambrock et al. (2013) indicate that garnet colours are determined by the transition ions occupying the dodecahedral X and octahedral Y sites.  $Mn^{+2}$  and  $Fe^{+2}$  cations in the X site and  $Fe^{+3}$ ,  $Mn^{+3}$ ,  $V^{+3}$  and  $Cr^{+3}$  cations in the Y site are described as transition elements or chromophores giving the colour to garnet crystals (Runciman and Marshall, 1975). The greenish colour could be attributed to the constituents  $Fe^{3+}$ ,  $Mn^{3+}$ ,  $Cr^{3+}$  and  $V^{3+}$  in the octahedral Y site. The reddish-brown colours could be ascribed to constituents  $Fe^{2+}$  in the dodecahedral X site and  $Mn^{3+}$  and  $Ti^{3+}$  in octahedral Y site (Fritsch and Rossman, 1993). The composition of solid-solution systems such as the grossular-andradite binary system may be very sensitive to small changes in the hydrothermal fluid composition (Jamtveit, 1991). There are significant rimward decreases in the Mn, Al, and Mg contents of the Hisarlıkaya garnet crystals. Jamtveit et al. (1993) suggest that decreasing and increasing element concentrations in skarn garnets might be caused by changes in the hydrothermal fluid composition during garnet growth and processes occurring near the garnet-fluid interface. These compositional changes could be attributed to the hydrothermal fluid variations due to the competition between external (infiltration) control and internal control by local mineral reactions (Jamtveit et al., 1993). During skarn formation, the grossular-rich cores were primarily

controlled by the local mineral assemblage of the magmatic intrusion and surrounding rocks, low crystal growth rate, and limited hydrothermal fluid infiltration (Jamtveit and Hervig, 1994). Accordingly, substantial  $Fe^{3+}$  rich fluid must infiltrate into the system in the late stage of metasomatism to form rims with high andradite contents. Based on this result, it can be concluded that these studied garnets display compositional zonation and colour changes due to the hydrothermal fluid transportation and also to the processes occurring between the magmatic intrusion and calcareous basement rocks during metasomatism in the Hisarlıkaya region.

These garnet crystal samples display dodecahedron-trapezohedron crystal habits, and also optical isotropic character. Their refractive indices are high ( $>1.78$ ), specific gravities range from 3.66 to 3.67 g/cm<sup>3</sup> and they are translucent, transparent, and glassy. They all possess similar physical properties, crystal forms, and chemical composition. According to standard gemmological tests, Hisarlıkaya garnet crystals may be considered as gemstones based on the mineralogical and gemmological characteristics but most of them are not appropriate for cutting and processing as gemstones due to their sizes and the presence of fractures and growth channels.

#### Acknowledgments

We are grateful to Dr. Abidin Temel, Aslihan Korkmaz, Dr. Fuat Erkül, and Osman Küçük Kurt for contributions during field studies, to Dr. Evren Çubukcu and Mehmet Özcan for generous support during scanning electron microscope studies, to Gülay Kiliç for support in completing XRD analyses, to Dr. Yusuf Kağan Kadioğlu and Dr. Kıymet Deniz for contributions to Confocal Raman spectrometry, to Dr. Koray Sözeri for standard gemmological tests and to Dr. Özgür Karaoğlu and Catherine Yiğit for English proofreading. We thank the editors and anonymous reviewers for their valuable comments and suggestions for improving the manuscript.

#### References

- Adamo I, Gatta GD, Rotiroti N, Diella V, Pavese A (2011). Green andradite stones: Gemmological and mineralogical characterisation. *European Journal of Mineralogy* 23: 91-100. doi: 10.1127/0935-1221/2011/0023-2079
- Akyürek B, Duru M, Sütçü YF, Papak İ, Şaroğlu Fet al. (1995). 1:100 000 scale geological map of Turkey, Ankara – F15 sheet-no:55. Maden Tetkik ve Arama Genel Müdürlüğü Ankara, Turkey.
- Alıcı P, Temel A, Gourgaud A, Kieffer G, Gündoğdu MN (1998). Petrology and geochemistry of potassic rocks in the Gölcük area (Isparta, SW Turkey): genesis of enriched alkaline magmas. *Journal of Volcanology and Geothermal Research* 85 (1-4): 423-446. doi: 10.1016/S0377-0273(98)00065-1
- Alıcı Şen P, Temel A, Gourgaud A (2002). Petrogenetic modelling of Quaternary post-collisional volcanism: a case study of central and eastern Anatolia. *Geological Magazine* 141 (1): 81-98. doi: 10.1017/S0016756803008550
- Amthauer G, Rossman GR (1998). The hydrous component in andradite garnet. *American Mineralogist* 83: 835-840. doi: 10.2138/am-1998-7-815
- Anders E, Grevesse N (1989). Abundances of the elements: Meteoritic and solar. *Geochimica et Cosmochimica Acta* 53 (1): 197-214. doi: 10.1016/0016-7037(89)90286-X

- Bocchio R, Adamo I, Diella V (2010). Trace-element profiles in gem-quality green andradite from classic localities. *Canadian Mineralogist* 48: 1205-1216. doi: 10.3749/canmin.48.5.1205
- Deer WA, Howie RA, Zussman J (1992). *An Introduction to the Rock Forming Minerals*. Essex, UK: Addison Wesley Longman Ltd, pp. 696.
- Dietl C (1999). Emplacement of the Joshua Flat Beer Creek Pluton (White-Inyo Mountains, California): a story of multiple material transfer processes, in Castro. *Geological Society of London: Special Publication*, 168: pp. 161-176.
- Dingwell DB, Brearley M (1985). Mineral chemistry of igneous melanite garnets from analcite-bearing volcanic rocks, Alberta, Canada. *Contributions to Mineralogy and Petrology* 90: 29-35. doi: 10.1007/BF00373038
- Fei X, Zhang Z, Cheng Z, Santosh M (2019). Factors controlling the crystal morphology and chemistry of garnet in skarn deposits: a case study from the Cuihongshan polymetallic deposit, Lesser Xing'an Range, NE China. *American Mineralogist* 104: 1455-1468. doi: 10.2138/am-2019-6968
- Fritsch E, Rossman GR (1993). The causes of color in garnets (abstract). *Friends of Mineralogy, Symposium, Tucson, AZ. Mineralogical Record* 24: 63.
- Gaspar M, Knaack C, Meinert LD, Moretti R (2008). REE in skarn system: A LA-ICP-MS study of garnet from the Crown Jewel gold deposit. *Geochimica et Cosmochimica Acta* 72: 185-205.
- Geiger CA, Rossman GR (2018). IR spectroscopy and OH-in silicate garnet: The long quest to document the hydrogarnet substitution. *American Mineralogist* 103: 384-393. doi: 10.2138/am-2018-6160CCBY
- Gilbertson A (2016). Value factors, design, and cut quality of colored gemstones (non-diamond). *The Gem Guide*: 1-8.
- Gomes CB (1969). Electron microprobe analysis of zoned melanites. *The American Mineralogist* 54: 1654-1661.
- Gwalani LG, Rock NMS, Ramasamy R, Griffin BJ, Mitchell BPM (2000). Complexly zoned Ti-rich melanite-schorlomite garnets from Ambadungar carbonatite-alkalic complex, Deccan Igneous Province, Gujarat State, Western India. *Journal of Asian Earth Science* 18: 163-176. doi: 10.1016/S1367-9120(99)00053-X
- Hofmeister AM, Chopelas A (1991). Vibrational spectroscopy of end-member silicate garnets. *Physics and Chemistry of Minerals* 17: 503-526. doi: 10.1007/BF00202230
- Jamtveit B (1991). Oscillatory zonation patterns in hydrothermal grossular-andradite garnets: Nonlinear behavior in regions of immiscibility. *American Mineralogist* 76: 1319-1327. doi: 10.2138/am-1991-004x/91/0708-1319\$02.00
- Jamtveit B, Andersen TB (1992). Morphological instabilities during rapid growth of metamorphic garnets. *Physics and Chemistry of Minerals* 19: 176-184. doi: 10.1007/BF00202106
- Jamtveit B, Wogelius RA, Frase DG (1993). Zonation patterns of skarn garnets: records of hydrothermal system evolution. *Geology* 21: 113-116. doi: 10.1130/0091-7613
- Jamtveit B, Hervig RL (1994). Constraints on transport and kinetics in hydrothermal systems from zoned garnet crystals. *Science* 263: 505-507.
- Jiang W, Li H, Evans NJ, Wu J, Cao J (2018) Metal sources of world-class polymetallic W-Sn skarns in the Nanling Range, South China: granites versus sedimentary rocks? *Minerals* 8 (265): 1-20. doi: 10.3390/min8070265
- Johnson ML, Boehm E, Krupp H, Zang JW, Kammerling RC (1995). Gem-quality grossular-andradite: e new garnet from Mali. *Gems&Gemology* 31 (3): 152-166.
- Keller J, Jung D, Eckhardt FJ, Kreuzer H (1992). Radiometric ages and chemical characterisation of the Galatean andesite massif Pontus, Turkey. *Acta Vulcanol Marinelli* 2: 267-276.
- Koçyiğit A, Lünel T (1987). Geology and tectonic setting of Alçı region, Ankara. *METU Journal of Pure Applied Sciences* 20: 35-59.
- Kolesov BA, Geiger CA (1998). Raman spectra of silicate garnets. *Physics and Chemistry of Minerals* 25:142-151. doi: 10.1007/s002690050097
- Lacivita V, D'Arco P, Orlando R, Dovesi R, Meyer A (2013) Anomalous birefringence in andradite-grossular solid solutions: a quantum-mechanical approach. *Physics and Chemistry of Minerals* 40: 781-788. doi: 10.1007/s00269-013-0612-6
- McAloon BP, Hofmeister AM (1995). Single-crystal IR spectroscopy of grossular-andradite garnet. *American Mineralogist* 80: 1145-1156. doi: 10.2138/am-1995-11-1205
- Meinert LD, Dipple GM, Nicolescu S (2005). World skarn deposit. In: Hedenquist JW, Thompson JFH, Goldfarb RJ, Richards JP (editors.), *Economic Geology 100th Anniversary Volume 1905-2005*. Amsterdam, The Netherlands: Elsevier Science B.V., pp. 299-336.
- Notsu K, Fujitani T, Ui T, Matsuda J, Ercan T (1995). Geochemical features of collision-related volcanic rocks in central and eastern Anatolia, Turkey. *Journal of Volcanology and Geothermal Research* 64: 171-192. doi: 10.1016/0377-0273(94)00077-T
- O'Donogh M (2006). *Gems*. 6th ed. Oxford, UK: Butterworth-Heinemann.
- Okay A, Tüysüz O (1999). *Tethyan Sutures of Northern Turkey*. London, UK: Geological Society, Special Publications. doi: 10.1144/GSL.SP.1999.156.01.22
- Payne T (1981). The andradites of San Benito County, California. *Gems&Gemology* 17 (3): 157-160.
- Ramasamy R (1986). Titanium-bearing garnets from alkaline rocks of carbonatite complex of Tiruppattur, Tamil Nadu. *Current Science* 55: 1026-1029.
- Rojay B, Süzen L (1997). Tectonostratigraphic evolution of the cretaceous dynamic basins on accretionary ophiolitic melange prism, SW of Ankara Region. *TPJD Bülteni* 9 (1): 1-12. (in Turkish with English abstract).

- Rubatto D, Burger M, Lanari P, Hattendorf B, Schwarz G et al. (2020). Identification of growth mechanisms in metamorphic garnet by high-resolution trace element mapping with LA-ICP-TOFMS. *Contributions to Mineralogy and Petrology* 175 (61): 1-19. doi: 10.1007/s00410-020-01700-5
- Runciman WA, Marshall M (1975). The magnetic circular dichroism of pyrope-almandine garnets. *American Mineralogist* 60: 1122-1124.
- Russell JK, Dipple GM, Lang JR, Lueck B (1999). Major-element discrimination of titanium andradite from magmatic and hydrothermal environments; an example from the Canadian Cordillera. *European Journal of Mineralogy* 11 (6): 919-935.
- Schmitt AC, Tokuda M, Yoshiasa A, Nishiyama T (2019). Titanian andradite in the Nomo rodingite: Chemistry, crystallography, and reaction relations. *Journal of Mineralogical and Petrological Sciences* 114: 111-121.
- Shannon D (1976). Revised effective ionic radii and systematic studies of interatomic distance in halides and chalcogenides. *Acta Crystallographica* 32: 751-767.
- Stubna J, Bacík P, Fridrichová J, Hanus R, Illášová L et al. (2019). Gem-quality green Cr-bearing andradite (var. Demantoid) from Dobšiná, Slovakia. *Minerals* 9 (164): 1-12.
- Tankut A, Wilson M, Yihunie T (1998). Geochemistry and tectonic setting of Tertiary volcanism in the Güvem area, Anatolia, Turkey. *Journal of Volcanology and Geothermal Research* 85: 285-301. doi: 10.1016/S0377-0273(98)00060-2
- Temel A (2001). Post-collisional Miocene alkaline volcanism in the Oğlakçı Region, Turkey: petrology and geochemistry. *International Geology Review* 43: 640-660. doi: 10.1080/00206810109465038
- Temel A, Yürür T, Alıcı P, Varol E, Gourgaud A, Bellon H, Demirbağ H (2010). Alkaline series related to Early-Middle Miocene intra-continental rifting in a collision zone: an example from Polatlı, Central Anatolia, Turkey. *Journal of Asian Earth Science* 38: 289-306. doi: 10.1016/j.jseas.2009.12.017
- Varol E, Temel A, Gourgaud G, Bellon H (2007). Early Miocene adakite-like volcanism in the Balkuyumcu region, central Anatolia, Turkey: Petrology and geochemistry. *Journal of Asian Earth Sciences* 30: 613-628. doi: 10.1016/j.jseas.2007.02.002. doi: 10.1016/j.jseas.2007.02.002
- Varol E, Temel A, Gourgaud G (2008). Textural and compositional evidence for magma mixing in the evolution of the Çamlıdere Volcanic Rocks (Galatean Volcanic Province), Central Anatolia, Turkey. *Turkish Journal of Earth Sciences* 17: 709-727.
- Varol E, Temel A, Yürür T, Gourgaud A, Bellon H (2014). Petrogenesis of the Neogene bimodal magmatism of the Galatean Volcanic Province, Central Anatolia, Turkey. *Journal of Volcanology and Geothermal Research* 280 (1): 14-29. doi: 10.1016/j.jvolgeores.2014.04.014
- Wang Y, Sun Q, Duan D, Bao X, Liu X (2019). The Study of crystal structure on Grossular-Andradite solid solution. *Minerals* 9 (11) 1-17. doi: 10.3390/min9110691
- Wilson M, Tankut A, Güleç N (1997). Tertiary volcanism of the Galatia province, northwest Central Anatolia, Turkey. *Lithos* 42: 105-121. doi: 10.1016/S0024-4937(97)00039-X
- Zamanian H, Sameti M, Pazoki A, Barani N, Ahmadnejad F (2017). Thermobarometry in the Sarvian Fe-skarn deposit (Central Iran) based on garnet-pyroxene chemistry and fluid inclusion studies. *Arabian Journal of Geosciences*, 10 (54): 1-16. doi: 10.1007/s12517-016-2785-z